MULTI-OBJECTIVE OPTIMIZATION OF A BOTTOMING ORGANIC RANKINE CYCLE (ORC) OF GASOLINE ENGINE USING SWASH-PLATE EXPANDER

J. Galindo, H. Climent, V. Dolz[1], L. Royo-Pascual

CMT – Motores Térmicos, Universitat Politècnica de València, Spain

Abstract

This paper presents a mathematical model of a bottoming Organic Rankine Cycle coupled to a 2l turbocharged gasoline engine to optimize the cycle from a thermo-economic and sizing point of view. These criteria were optimized with different cycle values. Therefore, a methodology to optimize the ORC coupled to Waste Heat Recovery systems in vehicle applications is presented using a multi-objective optimization algorithm. Multi-objective optimization results show that the optimum solution depend on the importance of each objective to the final solution. Considering thermo-economic criteria as the main objective, greater sizes will be required. Considering sizing criteria as the main objective, higher thermo-economic parameters will be obtained. Therefore, in order to select a single-solution from the Pareto frontier, a multiple attribute decision-making method (TOPSIS) was implemented in order to take into account the preferences of the Decision Maker. Considering the weight factors 0.5 for Specific Investment Cost (SIC), 0.3 for the area of the heat exchangers (A_{tot}) and 0.2 for Volume Coefficient (VC) and the boundaries of this particular application, the result is optimized with

[1] V. Dolz. CMT-Motores Térmicos, Universitat Politècnica de Valencia, Camino de Vera s/n, 46022 Valencia, Spain. Phone: +34 963877650 Fax: +34 963877659 e-mail: vidolrui@mot.upv.es

values of 0.48 m^2 (A_{tot}), 2515 €/kW (SIC) and 2.62 MJ/m^3 (VC). Moreover, the profitability of the project by means of the Net Present Value and the Payback has been estimated.

Keywords

Organic Rankine Cycle, Gasoline engine, Waste Heat Recovery, Optimization analysis, Genetic Algorithm, TOPSIS

NOMENCLATURE

Acronyms

EG	Exhaust gas
GA	Genetic Algorithm
ICE	Internal Combustion Engines
LMTD	Logarithmic Mean Temperature Difference
NPV	Net Present Value
ORC	Organic Rankine Cycle
PB	Payback
SFC	Specific Fuel Consumption
SIC	Specific Investment Cost
SP	Size Parameter
TCC	Total Component Costs

TOPSIS	Technique for Order Preference by Similarity to an Ideal Solution
VC	Volume Coefficient
WHR	Waste Heat Recovery
WMM	Weighted Metric Method

Notation

Latin

A	Area	m^2
C	Cost	€
C_p	Specific Heat Capacity at constant pressure	J/kgK
d	Diameter	m
D_h	Hydraulic diameter	m
f	Friction factor	-
fc	Fuel consumption	kg/h
G	Mass flow velocity	kg/m^2s
h	Specific enthalpy	kJ/kg
hr	Hours	h
K	Thermal conductivity	W/mK

L	Lenght	m
$\dot{m}$	Mass flow	kg/s
N	Number of plates	-
P	Pressure	bar
$\dot{Q}$	Thermal power	kW
r	Discount rate	-
S	Saving	€
SH	Superheating temperature	ºC
t	Number of periods	-
T	Temperature	°C
U	Heat transfer coefficient	W/m^{2}K
v	Specific volume	m^3/kg
$\dot{V}$	Volumetric flow	m^3/s
Vol	Volume	l
W	Width	m
$\dot{W}$	Mechanical power	kW
X_{tt}	Martinelli Parameter	-

33 Greek letters

ε	Exergetic efficiency	-
η	Isentropic efficiency	-
Δ	Increment	
ρ	Density	kg/m^3
μ	Dynamic viscosity	
Δ	Increment	

34 Subscripts

$1-8$	State points
et	Ethanol
eg	Exhaust gas
pl	Plate
A	Zone A
B	Zone B
C	Zone C
tot	Total
NcB	Nucleate Boiling
cv	Convective Boiling

l	Liquid
fg	Liquid to gas
v	Vapour
e	Effective
eq	Equivalent
tp	Two Phase
ave	Average
$wall$	Wall
in	Inlet conditions
out	Outlet conditions
is	Isentropic
exp	Expander
p	Pump
c	Condenser
b	Boiler
net	Net
$pipe$	Pipe
lab	Labour

cp	Components
cs	Consumption
eng	Engine
f	Fuel

Dimensionless numbers

$Co = \left(\frac{\rho_g}{\rho_l}\right) * \left(\frac{1 - X_m}{X_m}\right)^{0.8}$	Convection number
$Fr = \frac{G^2}{\rho_l^2 * g * D_h}$	Froude number
$Bo = \frac{q}{G * i_{fg}}$	Boiling number
$Pr = \frac{\mu_l * C_{p,l}}{k_l}$	Prandtl number
$Re = \frac{D_h * V_{TP} * \rho_l}{\mu_l}$	Reynolds number

1. Introduction

Increasingly regulation targets on diesel emissions are supposed to be imposed in the EU during the forthcoming years to reach the target of carbon dioxide emissions lower than 95 g CO_2/km in year 2020 [1]. In order to fulfill these limits, improvements in vehicle consumption have to be achieved [2]. The automotive ICE, despite its technological advances over the years, converts just around 15-32% of the fuel energy into mechanical energy. Most of the total energy is lost through the exhaust gas and coolant in form of heat, and part of that energy could be recovered to produce electrical or mechanical power. Therefore, these sources can be exploited to improve the overall efficiency of the engine. Between these sources, exhaust gases show the largest potential of WHR due to its high level of exergy [3]. Between WHR technologies Rankine cycles are considered as the most promising candidates for improving diesel engines [4]. Simplicity and availability are two of the main advantages of this system.

Most of investigations for ORC are focused on configuration optimization and single-optimization in ICEs waste heat recovery problems [5]–[7],[8]. However, several authors revealed that multi-objective optimization and multi-parameters solutions are advisable to achieve the best overall thermodynamic and economic performance for the subcritical ORC [9]–[12]. In order to fulfill optimization requirements, genetic algorithms (GA) have been extensively adopted for low grade waste heat recovery problems. Most of them corresponds to ORC applied to industrial installations [13]. Only a few have been applied to IC engines [14]. However, no bottoming ORC coupled to an ICE has been analyzed and evaluated using this method, taking account thermo-economic and sizing criteria. Moreover, values of real experimental tests have been used to calibrate this model. In a previous paper [15], five engine steady-state operating points have been tested using ethanol as working fluid and a swash-plate expander as expander machine. A model of the installation has been developed by the authors with maximum deviation of 4% regarding pressures and temperatures and a value of 5% regarding torque [16]. This model has been used as a reference validation of the mathematical model proposed in this article.

In this paper, a thermo-economic model of the ORC system coupled to a gasoline engine is presented. This model is based on energy balances and economic criteria of the different components of the ORC system. The main objective of this work is to evaluate this thermo-economic model as a tool to optimize a multi-objective problem using a Genetic Algorithm.

2. Description of the ORC

Fig 1 and Fig 2 shows respectively the schematic diagram and the experimental installation of the ORC cycle. Red lines correspond to the exhaust gas line. The ethanol cycle loop is divided in two colors, green in the high pressure level and black in the low pressure level. Cooling loop is defined by blue lines (dark blue for the inlet cooling line and light blue for the outlet cooling line).

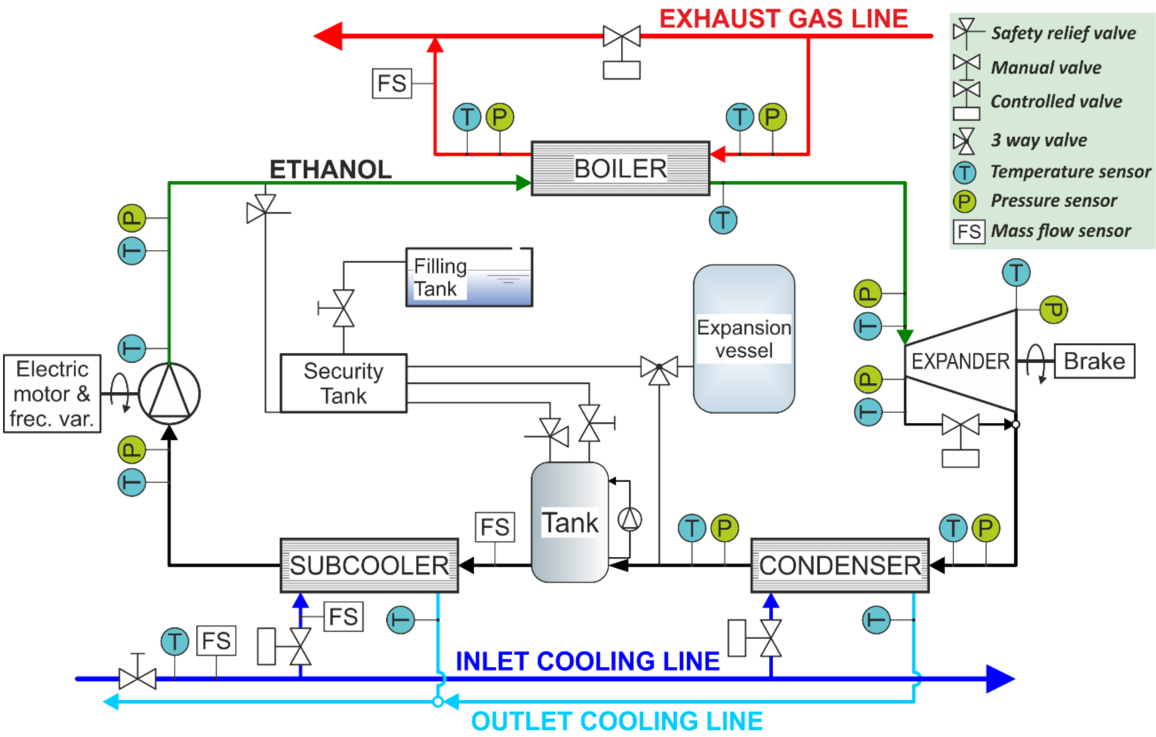

Fig 1. Schematic diagram of the installation

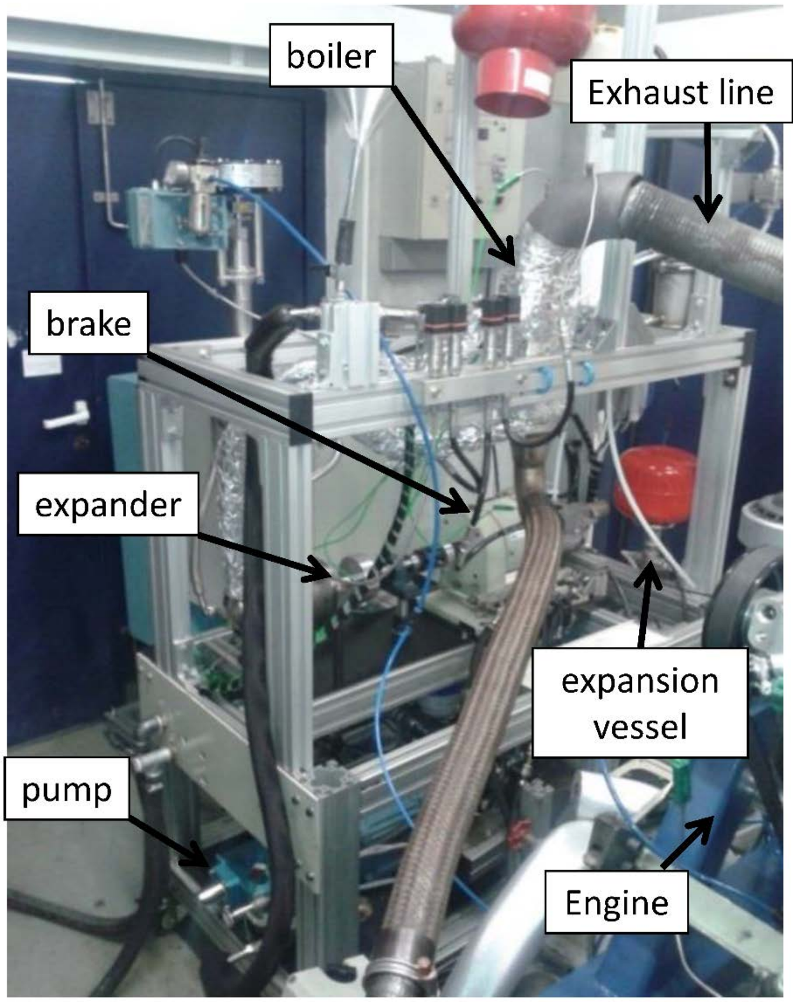

Fig 2. ORC Mock-up

The heat needed to vaporize the ethanol is provided by the engine exhaust gases. First of all, the working fluid is pumped from the tank at the condensing pressure to the boiler at the evaporating pressure. Then, the working fluid is pre-heated, vaporized and superheated in the heat exchanger. The ethanol vapor expands from the evaporating pressure to the condensing pressure in the expander machine. Finally, low pressure vapor is extracted from the expander and flows to the condenser, where it condenses using cooling water. The boiler ensures the heat transfer from exhaust gas to the working fluid. The condenser is followed by an expander vessel in order to impose the low pressure in the installation and a liquid reservoir. The expander prototype is a piston swash-plate.

Fig 3 shows a simplified diagram of the ORC designed for a waste heat recovery application. References to this diagram will be made during the whole article. The main elements of the cycle (boiler, expander, condenser and a pump) are presented in this figure. Boiler and condenser are divided in three areas, corresponding to single-phase liquid, two phase and single-phase vapor.

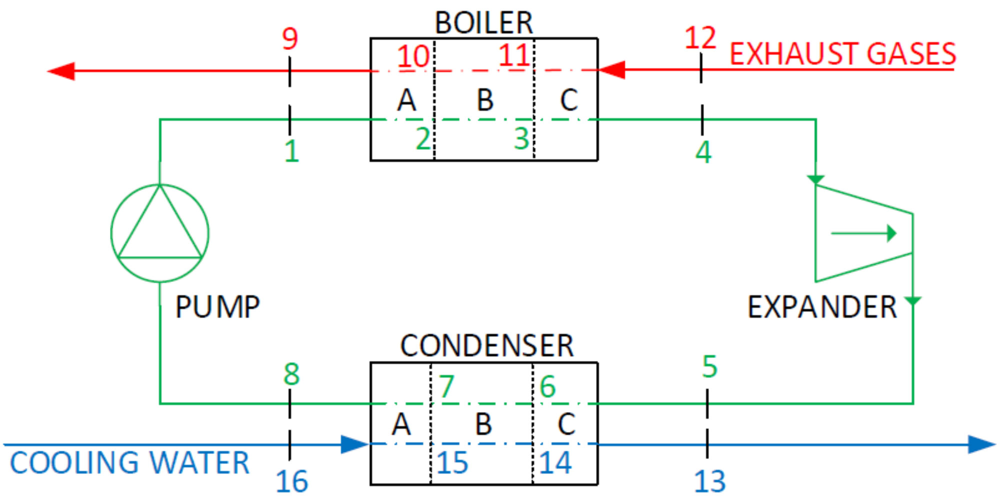

Fig 3. Cycle diagram for thermodynamic analysis

Fig 4 shows the ethanol T-S diagram. Points from 1 to 8 indicate the ethanol cycle, points 9 to 12 indicate the exhaust gas cooling process and points from 13 to 16 indicate the water heating process.

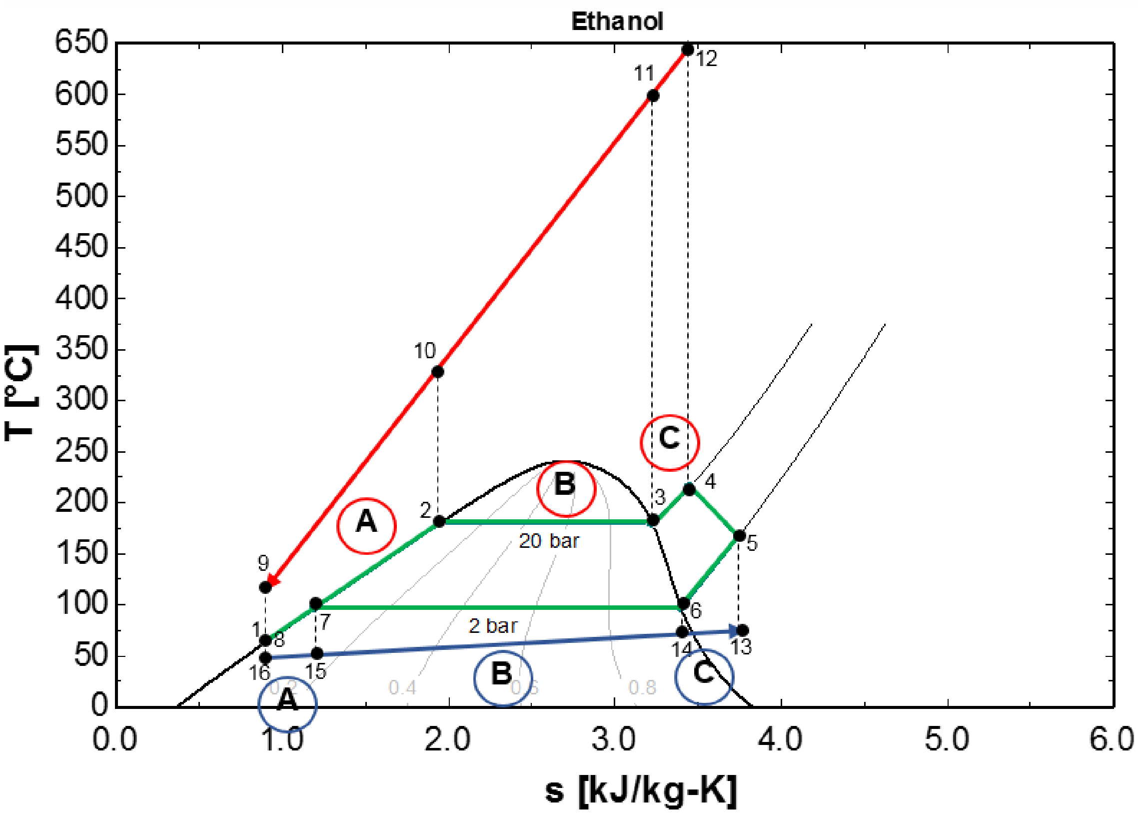

Fig 4. T-S ethanol diagram with state points

3. Mathematical model

A thermodynamic model of a bottoming ORC is used to evaluate the performance of the system.

3.1. Boiler and condenser model

Plate heat exchangers are modeled by means of the Logarithmic Mean Temperature Difference (LMTD), considering a three-zone approach. Each of them is characterized by a heat transfer coefficient (U) and area (A).

The evaporator geometric parameters are presented in Table 1. Geometric parameters of the condenser are the same as the evaporator, except for the width, which is 0.4 m.

Table 1. Boiler geometric parameters

Parameter	Description	Value
D_h=2a	Hydraulic diameter	0.008 m
W	Width	0.1 m
L	Length	0.4 m
d_{pl}	Thickness plate	0.002 m
β	Chevron angle	45º
K_{pl}	Thermal conductivity	14.9 W/mK

The heat transfer coefficient of a plate heat exchanger is computed as:

$$\frac{1}{U} = \frac{1}{h_{et}} + \frac{1}{h_{eg}} + \frac{d_{pl}}{k_{pl}} \qquad (1)$$

Where h_{et} and h_{eg} are the convective heat transfer in the ethanol and the exhaust gas side respectively, d_p is the thickness of the plate and k_{pl} is the thermal conductivity of the plate. Fouling resistances are neglected because it is assumed new plate heat exchangers.

The total heat exchanger area in each heat exchanger (boiler and condenser) is the sum of each zone (A, B and C in Fig 4):

$$A_{tot} = A_A + A_B + A_C = \left(N_{pl} - 2\right) * L * W \qquad (2)$$

Where A_{tot} is the total heat transfer area, N_{pl} is the number of plates, L and W are the length and width of the plate exchanger respectively.

3.1.1. Single phase (zones A and C)

For the convective heat transfer (Eq. 3) and pressure drop (Eq. 4 and 5) in the single phase Thonon correlation [17] was used:

$$Nu = 0.299 * Re^{0.645} * Pr^{\frac{1}{3}} \tag{3}$$

$$f = 0.685 * Re^{-0.172} \tag{4}$$

$$\Delta P = \frac{2 * f * G^2}{\rho * D_h} * L \tag{5}$$

Where f is the friction factor, G is the mass flow velocity, ρ is the mean fluid density, D_h is the hydraulic diameter and L is the length of the plate exchanger.

3.1.2. Boiling heat transfer coefficient (zone B in boiler)

The boiling heat transfer coefficient is estimated by Chen [18] correlation. This heat exchange coefficient takes into account two mechanisms: an effective Reynolds number factor (F) and a bubble-growth suppression factor (S). The first factor (F) is the ratio of the two-phase Reynolds number to the liquid Reynolds number and it is assumed as a function of the Martinelli parameter X_{tt} [19]. The second one (S) was defined as the ratio of the effective superheat to the total superheat of the wall. These two functions were determined empirically from experimental data.

$$h_{tp} = S * h_{NcB} + F * h_{cv} \tag{6}$$

$$h_{NcB} = 0.00122 * \frac{k_l^{0.79} * Cp_l^{0.45} * \rho_l^{0.49} * g^{0.25}}{\sigma^{0.5} * \mu_l^{0.29} * h_{fg}^{0.24} * \rho_v^{0.24}} * \Delta T^{0.24} * \Delta P^{0.75} \tag{7}$$

$$h_{cv} = 0.023 * Re_l^{0.8} * Pr_l^{0.4} * \frac{k_l}{D_h} \tag{8}$$

$$F = \left(\frac{Re}{Re_l}\right)^{0.8} \tag{9}$$

$$S = \left(\frac{\Delta T_e}{\Delta T}\right)^{0.99} \tag{10}$$

Where k is the thermal conductivity, σ is the surface tension, μ is the dynamic viscosity, h_{fg} is the latent heat of vaporization, ΔT_e is the effective superheat with flow, ΔT is the superheat and ΔP is the difference in vapor pressure corresponding to ΔT.

Pressure drop is computed with the same equation as the single phase (Eq. 5), using Hsieh correlation [20] to obtain the friction factor in the boiling phase.

$$f = 61000 * Re_{eq}^{-1.25} \tag{11}$$

Where Re_{eq} is the equivalent Reynolds number regarding the flow as a liquid.

3.1.3. Condensation heat transfer coefficient (zone B in condenser)

The condensation heat transfer coefficient and friction factor (pressure drop) are estimated by Kuo [21] correlation. This correlation has been developed for vertical plate heat exchangers using R410A. Results are similar to Shah correlation developed for ethanol inside pipes [22].

$$h_{tp} = h_l * \left(0.25 * Co^{-0.45} * Fr_l^{0.25} + 75 * Bo^{0.75}\right) \tag{12}$$

$$h_l = 0.2092 * \left(\frac{k_l}{D_h}\right) * Re_l^{0.78} * Pr_l^{\frac{1}{3}} * \left(\frac{\mu_{ave}}{\mu_{wall}}\right)^{0.14} \tag{13}$$

$$f = 21500 * Re_{eq}^{-1.14} * Bo^{-0.085} \quad (14)$$

Where Co, Fr, Bo, Pr and Re are respectively the numbers of Convection, Froude, Boiling, Prandtl and Reynolds.

3.2. Expander model

The expander has been characterized by an isentropic efficiency. The maximum value of this isentropic efficiency is fixed by the built-in volumetric expansion ratio. Expander speeds below 3500 rpm (and therefore higher pressure ratios than optimal one) lead to an expander performance drop mainly due to the effect of leakages, whereas higher expander speed and lower pressure ratios lead to a sharply reduction in the expander isentropic efficiency mainly due to the effect of mechanical losses and intake pressure drop. For a given rotational speed and mass flow rate, the isentropic efficiency is function of the pressure ratio. This hypothesis has been assumed in order to simplify the model. Therefore, a typical isentropic process of a swash-plate expander in the pressure levels has been used from 20 to 40 bar [15]. The isentropic efficiency has been correlated as a function of the pressure ratio (Eq. 15) using experimental data with a correlation coefficient of 92.35%.

$$\eta_{iso} = f\left(\frac{P_{high}}{P_{low}}\right) \quad (15)$$

The characterization of the expander size has been made using the “Volume Coefficient” (VC) [23]. This expression takes into account the volumetric expansion ratio and constitutes a representative factor of the actual size of the volumetric machine.

$$VC = \frac{\dot{V}_{out}}{\dot{W}_{exp}} \tag{16}$$

Where $\dot{V}_{out}$ is the volumetric flow at the outlet of the expander and $\dot{W}_{exp}$ is the power delivered by the expander in the expansion process of the expander.

3.3. Pump model

The pump behavior has been characterized by its isentropic efficiency, which is assumed to be constant with a value of 80% as a representative efficiency value for these machines [24].

$$\eta_{iso} = \frac{h_{1s} - h_8}{h_1 - h_8} \tag{17}$$

3.4. Cycle model

The global cycle model is obtained by computing the energy balance equations to each component. The boundary conditions of the experimental tests presented in [15] have been imposed to the mathematical model (Temperatures and mass flows). Moreover, the efficiency of the expander as a function of the pressure ratio of the real experimental tests was also the input of the model. Therefore, in order to obtain the optimal point, sensitivity studies are presented using the evaporation pressure and the superheating.

Table 2 indicates a summary of these equations.

Table 2. Energy balance equations

Cycle component	**Energy balance equations**
Expander	$\eta_{is} = \frac{\dot{W}_{exp}}{\dot{W}_{exp,is}}, \dot{W}_{exp,is} = \dot{m}_{et} * (h_4 - h_{5s}), \dot{W}_{exp} = \dot{m}_{et} * (h_4 - h_5)$
Pump	$\eta_{is} = \frac{\dot{W}_{p,is}}{\dot{W}_p}, \dot{W}_{p,is} = \dot{m}_{et} * (h_{1s} - h_8), \dot{W}_p = \dot{m}_{et} * (h_1 - h_8)$
Condenser	$\dot{Q}_c = \dot{m}_{et} * (h_5 - h_8)$
Boiler	$\dot{Q}_b = \dot{m}_{et} * (h_4 - h_1)$

Using the thermodynamic properties of the state points, the net power (Eq. 18) and the cycle efficiency (Eq. 19) can be defined:

$$\dot{W}_{net} = \dot{W}_p - \dot{W}_{exp} \tag{18}$$

$$\eta_{ORC} = \frac{\dot{W}_{net}}{\dot{Q}_b} \tag{19}$$

Where $\dot{W}_{net}$ is the net power and η_{ORC} is the cycle efficiency.

3.5. Economic model

The thermodynamic mathematical model of the cycle, described in the previous paragraph, is expanded by considering costs of the main elements in the cycle. These costs are estimated from the work of Quoilin et al. [7] and they are presented in Table 3.

Table 3. Component costs

Component	Dependent variable	Cost [€]
Expander	Volume flow rate (m^3/s)	$1.5 * (225 + 170 * \dot{V}_{in})$
Boiler	Heat exchange area(m^2)	$1.5 * (190 + 310 * A_{tot})$
Condenser	Heat exchange area(m^2)	$190 + 310 * A_{tot}$
Pump	Pump power (W)	$900 * \left(\frac{\dot{W}_p}{300}\right)^{0.25}$
Liquid receiver	Volume (l)	$31.5 + 16 * Vol$
Piping	Pipe diameter (mm) Pipe length (m)	$(0.897 + 0.21 * d_{pipe}) * L_{pipe}$
Working fluid	Mass (kg)	$20 * M$
Hardware	-	300
Control system	-	500
Labor	Total component costs(€)	$0.5 * TCC$

As Quoilin et al. [7] consider in their work, the estimated cost of commercial volumetric compressors is multiplied by a factor of 1.5 to obtain the estimated cost of the volumetric expander, in order to consider the low level of maturity in the volumetric expander for these type of applications. In the case of the evaporator, which should withstand high temperatures in the exhaust gases side and high pressures and thermal stress in the ethanol side, the multiplying factor is also assumed to be 1.5. Diameters and lengths of pipes are measured in the experimental facility, in order to obtain representative values of these tubes. The total ethanol mass of the system is calculated from the real volume of ethanol in the installation and the density, assuming that half of the heat exchangers and the liquid receiver are filled with liquid and half with vapor.

One of the thermo-economic objective functions most used in the literature is the Specific Investment Cost (SIC) parameter in €/kW [25], which is defined in Eq. 20.

$$SIC = \frac{C_{lab} + C_{cp}}{\dot{W}_{net}} \tag{20}$$

Where C_{lab} is the cost of labour and C_{cp} is the cost of the components.

Moreover, the Net Present Value and Payback were estimated, defined in Eq. 21 and Eq.22.

$$NPV = \sum_{t=1}^{T} \frac{C_t}{(1+r)^t} - C_o \tag{21}$$

$$PB = \frac{C_o}{C_t} \tag{22}$$

Where C_t is the net cash inflow during the period t, C_o is the total investment costs, r is the discount rate and t is the number of periods.

The net cash inflow is computed using the specific fuel consumption in a particular engine operating point and estimate the operating hours of a vehicle in a year. The higher engine operating point (30 kW of thermal power) was used because it involves greater recovery potential from the exhaust.

$$SFC = \frac{fcs}{\dot{W}_{eng}} \tag{23}$$

$$S_{ORC} = SFC * \dot{W}_{net} \tag{24}$$

$$C_t = \left(\frac{S_{ORC} * hr_{year}}{\rho_f}\right) * C_f \tag{25}$$

Where f_{cs} is the fuel consumption in kg/h, $\dot{W}_{eng}$ is the engine power, SFC is the specific fuel consumption, hr_{year} is the number of operating hours of a vehicle in a year, ρ_f is the density of the fuel and C_f is the cost per liter of the fuel.

Although several thermodynamic and economic parameters have been presented in the previous section, three objective functions have been considered in order to simplify the optimization of the system: SIC in €/kW, heat exchangers area (sum of $A_{tot,b}$ and $A_{tot,c}$) in m^2 and expander size (VC) in $MJ/m^{3.}$ The Specific Investment Cost has been chosen as a global parameter of the thermo-economic behavior of the system. The remainder economic parameters (NPV and PB) are characterized by high degree of uncertainty due to the estimation of the fuel price (C_f) and the number of ORC operating hours during a year (hr_{year}). Therefore, in order to know the influence of these parameters two parametric studies are presented after the optimization of the system. In addition to SIC, two more sizing parameters were chosen to take into account both the size of the heat exchangers and the expander.

3.6. Assumptions

The main assumptions in analyzing the ORC are as follows:

- Pressure drop at the ethanol side is low comparing to the level of pressure in the system. Therefore, for this first approach they are neglected.
- The system works under steady state conditions.
- The heat source is exhaust gas at 678ºC, with mass flow rate of 48 g/s, corresponding to the 30 kW of thermal power in the boiler [15].
- The condenser is cooled with water at 50ºC, and a flow rate of 990 l/h.
- The superheating temperature at the expander inlet is 35ºC.
- The subcooling temperature after the condenser is 30 ºC.
- Boiler is vertical heat exchanger type and the condenser is a vertical plate heat exchanger.
- A discount rate of 4% and 10 years are fixed in the calculation of NPV and PB [26]. The cost of fuel is estimated to 1€/l.
- Total number of hours of the ORC is estimated to 1100h a year (3 hour each day).
- The model has been validated with experimental results in our ORC facility [15], and differences between model and experimental variables are lower than 5% [16].

4. Results

The goal of this study is to optimize the cycle using both thermo-economic criterion (SIC) and sizing criteria (Boiler-Condenser area and VC). In order to analyze the behavior of these criteria in different conditions of the cycle, a sensibility analysis is presented varying the main parameters of the cycle, which are the evaporating pressure and superheating temperature.

Fig 5 shows the net power, defined as the difference between expander and pump power in kW (Eq. 18) in grey scale, the SIC in €/kW (Eq. 20) in blue lines and Total costs in € (Sum of cost in Table 3) in red lines.

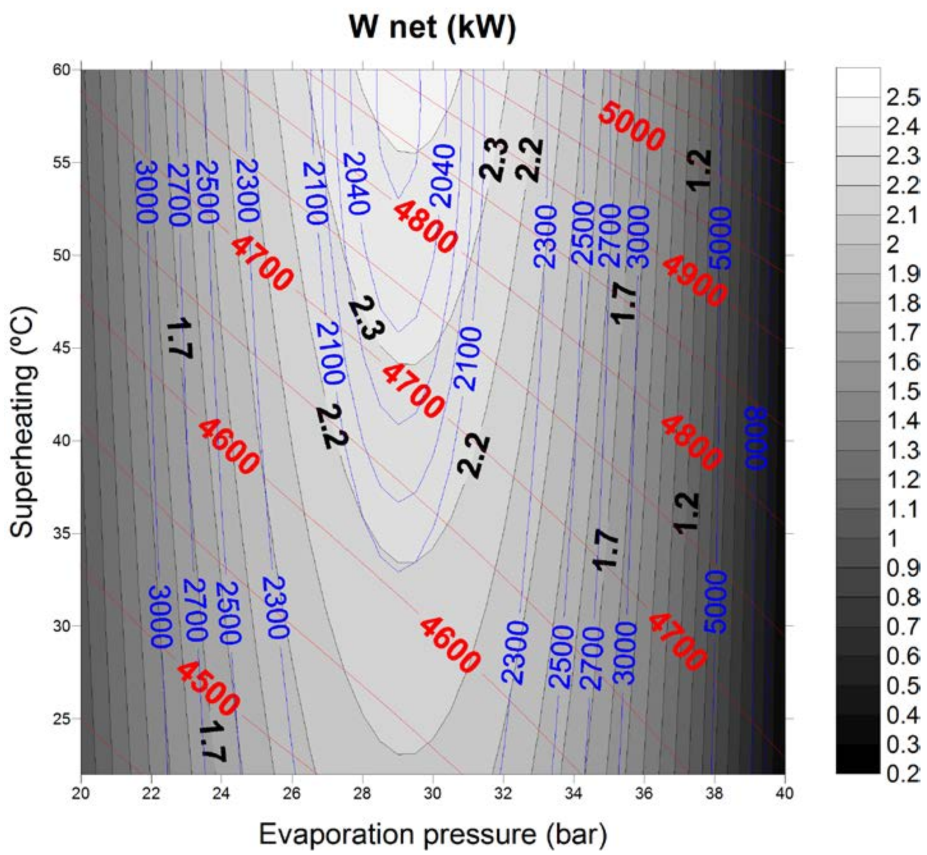

Fig 5. Net power in kW (grey scale), SIC in €/kW (blue lines) and total cost in € (red lines)

The isentropic efficiency of expander (Eq. 15) has an important effect on the level of pressure. When evaporation pressure is approx. 29 bar the expander works with an optimal expansion ratio and expander isentropic efficiency is maximum, consequently, maximum power is obtained from the cycle. Regarding superheating temperature, increasing its value produce higher enthalpy drop through the expander. Consequently, net power has a peak with evaporation pressure of approx. 29 bar and close to the superheating temperature of 60ºC. Maximum net power corresponds to 2.41 kW (in the same zone). Regarding Total costs, they increase with higher level of pressure and superheating temperature.

Fig 6 shows the Total Cost, defined as the sum of costs of Table 3 in grey scale. Purple lines corresponds to the cost of the pump in €, blue ones to the cost of the evaporator in € and green ones to the cost of the condenser in €.

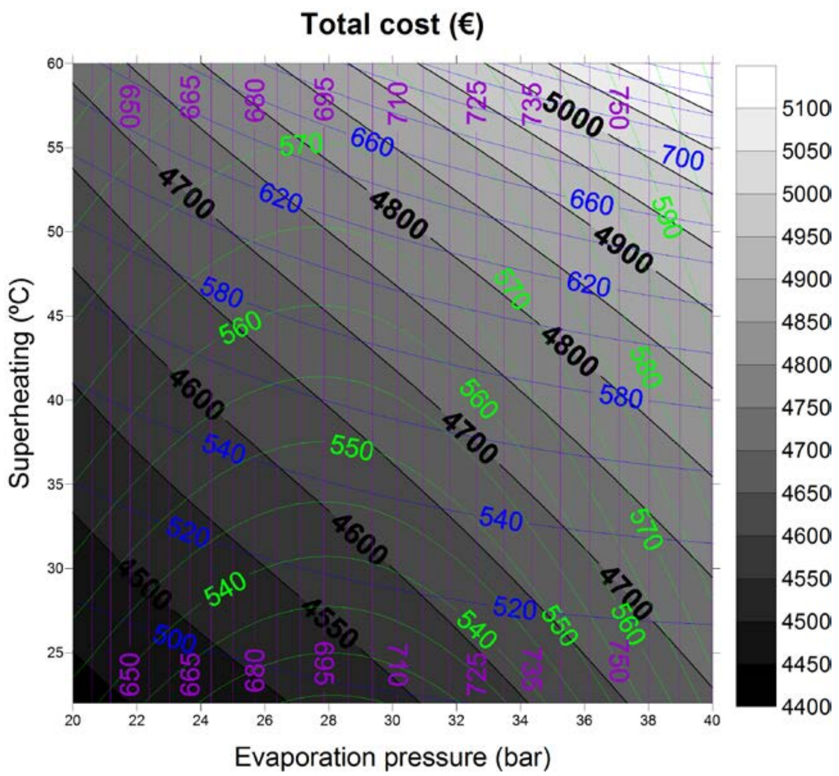

Fig 6. Total cost in € (grey scale) of elements in the ORC, cost of the pump in € (purple lines), cost of the boiler in € (blue lines) and cost of the condenser in € (green lines)

The cost of the pump is a function of the required power, therefore, considering constant mass flow values, it will increase with higher levels of pressure. The cost of the boiler increases with higher level of pressure and superheating temperature, however, the latter has further effect than the former as it can be seen in the direction of the lines with the same cost. The reason is that as pressure and superheating temperature increase, the pinch point temperature difference tends to decrease and therefore, to maintain this temperature difference, the heat transfer area in the boiler should increase. Regarding the condenser, it is similar to the boiler. However, in this particular case the expander isentropic efficiency has an effect on temperature at the inlet of the condenser.

As a final consequence, SIC parameter is optimized in this particular case at 28 bar and 60ºC of superheating temperature, with a cost of 2030 €/kW.

Regarding sizing criterion, three parameters are presented in Fig 7, which are Boiler area in m^2 (blue lines), the Volume Coefficient of the expander in MJ/m^3 (purple lines) and the condenser area in m^2 (green lines).

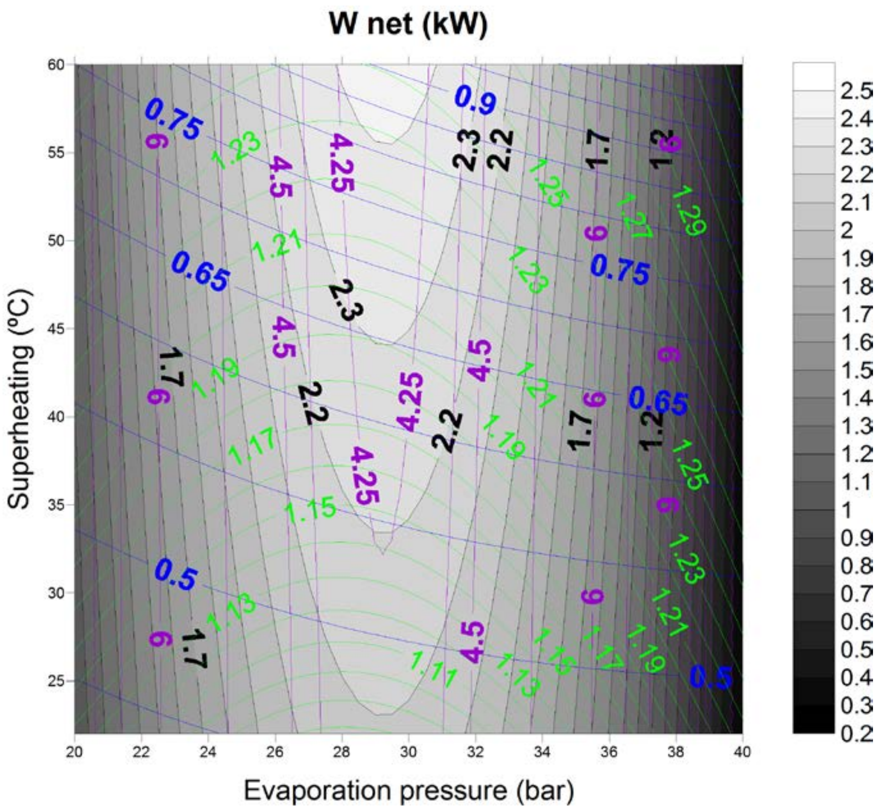

Fig 7. Net power in kW (grey scale), area of boiler in m^2 (blue lines), expander size (VC) in MJ/ m^3 (purple lines) and condenser in m^2 (green lines)

As previously stated, higher levels of pressure and temperature of the working fluid reduce the pinch point in the evaporator, increasing the heat exchange area in the boiler. The expander size (VC) increases slightly with superheating temperature with a similar trend to SIC. This parameter depends on the specific volume at the outlet of the expander and the work delivered by the expander. As the work delivered in the expander is strongly influenced by the expander isentropic efficiency, the optimal values for this parameter are close to the zone with maximum isentropic efficiencies. Higher superheating values implies higher volume flow rates at the outlet of the expander. Therefore, the result is a global increasing of the volume coefficient (VC) in the areas where the expander isentropic efficiency is minimum. Regarding the condenser, the area depends on the temperature at the outlet of the expander, which is a function of the expander isentropic efficiency. The tendency is similar to the boiler area behavior. Consequently, optimum volume coefficient is achieved at lower levels of superheating and pressures between 28 bar and 32 bar.

5. Optimization of the ORC using a genetic algorithm

The main parameters of the ORC have been changed using a multi-objective optimization algorithm in order to optimize the system from a thermo-economic and sizing point of view. In this study, VC, A_{tot} (sum of $A_{tot,b}$ and $A_{tot,c}$) and SIC are evaluated as objective functions as a function of the decision variables (Eq. 26, 27 y 28).

$$A_{tot} = f(P_1, P_5, SH, \dot{m}_{et}, T_9) \quad (26)$$

$$VC = f(P_1, P_5, SH, \dot{m}_{et}, T_9) \quad (27)$$

$$SIC = f(P_1, P_5, SH, \dot{m}_{et}, T_9) \quad (28)$$

Where P_1 is the evaporation pressure, P_5 is the condensation pressure, SH is the superheating temperature, $\dot{m}_{et}$ is the ethanol mass flow and T_9 is the temperature at the boiler outlet in the exhaust gas side (Fig 3). The multi-objective optimization problem of the ORC system is performed by using a GA in ModeFRONTIER. The parameters setting in the GA are shown in Table 4.

Table 4. Parameters of GA

Parameter	**Value**
Type of algorithm	MOGA-II[27]
Number of Generations	100
Probability of Directional Cross-Over	0.5
Probability of Selection	0.05
Probability of Mutation	0.1

Table 5 shows the upper and lower limits of the decision variables. These values correspond with technological limits of the ORC mock-up. Condensing pressure upper bound limit corresponds to safety valves value, evaporating pressure upper bound limit corresponds to the critical pressure of ethanol, superheating and ethanol mass flow are limited by the degradation and condensing temperature of ethanol and temperature at the outlet of the boiler in the EG side is limited to avoid condensation of water in the exhaust. Moreover, optimum values are far from these lower and upper bounds of the decision variables.

Table 5. Limits of decision variables

Decision variables	Lower bound	Upper bound
Evaporation pressure (bar)	10	60
Condensing pressure (bar)	2	4
Superheating temperature (ºC)	0	50
Ethanol mass flow (kg/s)	0.01	0.06
Outlet temperature EG (ºC)	100	200

Moreover, some restrictions were imposed to the GA:

- Pinch point in the boiler and the condenser should be greater than 10 °C and 5 °C respectively [28].
- Temperature at the outlet of the boiler (T_4 in Fig 4) should be lower than the ethanol degradation temperature. From our experience working with this fluid, it is approximately 250 °C.

The aim of a multi-objective optimization problem using this Genetic Algorithm is to find the Pareto frontier optimal solution. Each point of the frontier represents one potential solution in the multi-objective optimization problem. Therefore, any point is better than another in the frontier, just the improvement of one of them involves worsening the others. The selection of the final optimum depends on the importance of each objective. Fig 8, Fig 9 and Fig 10 show the different views of the optimization. Fig 8 shows A_{tot} vs SIC (VC in bubble color), Fig 9 shows A_{tot}

vs VC (SIC in bubble color) and Fig 10 shows VC vs SIC (A_{tot} in bubble color). The optimum solution depend on the importance of each objective:

- Considering SIC as the main objective, greater heat exchangers area will be required. Therefore, with an optimal value of SIC of 2264 €/kW, the heat exchangers area will be 0.67 m^2 and the Volumetric Coefficient 3.26 MJ/m^3. This value has been plotted in Fig 8, Fig 9 and Fig 10 using a green circle (point C).
- Considering sizing of the heat exchangers as the main objective, higher SIC will be obtained. Therefore, with an optimal value of area of 0.076 m^2, the SIC will be 5475 €/kW and the Volumetric Coefficient 4.16 MJ/m^3. This value has been plotted in Fig 8, Fig 9 and Fig 10 using an orange circle (point A).
- Considering sizing of the expander as the main objective, higher SIC and heat exchangers area will be obtained. Therefore, with an optimal value of VC of 2.22 MJ/m^3, the heat exchangers area will be 0.17 m^2 and SIC 3581 €/kW. This value has been plotted in Fig 8, Fig 9 and Fig 10 using a purple circle (point B).

Therefore, in order to select a single-solution from the Pareto frontier, a methodology [29] was implemented in order to take into account the preferences of the Decision Maker. The Technical for Order Preference by Similarity to an Ideal Solution (TOPSIS) [30] is applied to select the final solution on the Pareto Frontier. This method considers the distances to both positive ideal solution and negative ideal solution. In this method, the weight factor is defined for each optimization parameter. Considering the weight factors as 0.5 for SIC, 0.3 for A_{tot} and 0.2 for VC and the boundaries of this particular application (ORC coupled to a turbocharged engine), the result is optimized with values of 0.48 m^2 (A_{tot}), 2515 €/kW (SIC) and 2.62 MJ/m^3 (VC). The decision variables of this optimum were 47 bar (evaporation pressure), 3.3 bar (condensing pressure), 9 ºC (superheating temperature), 0.028 kg/s (ethanol mass flow) and 100 ºC (outlet temperature). This value has been plotted in Fig 8, Fig 9 and Fig 10 using a red circle (point D).

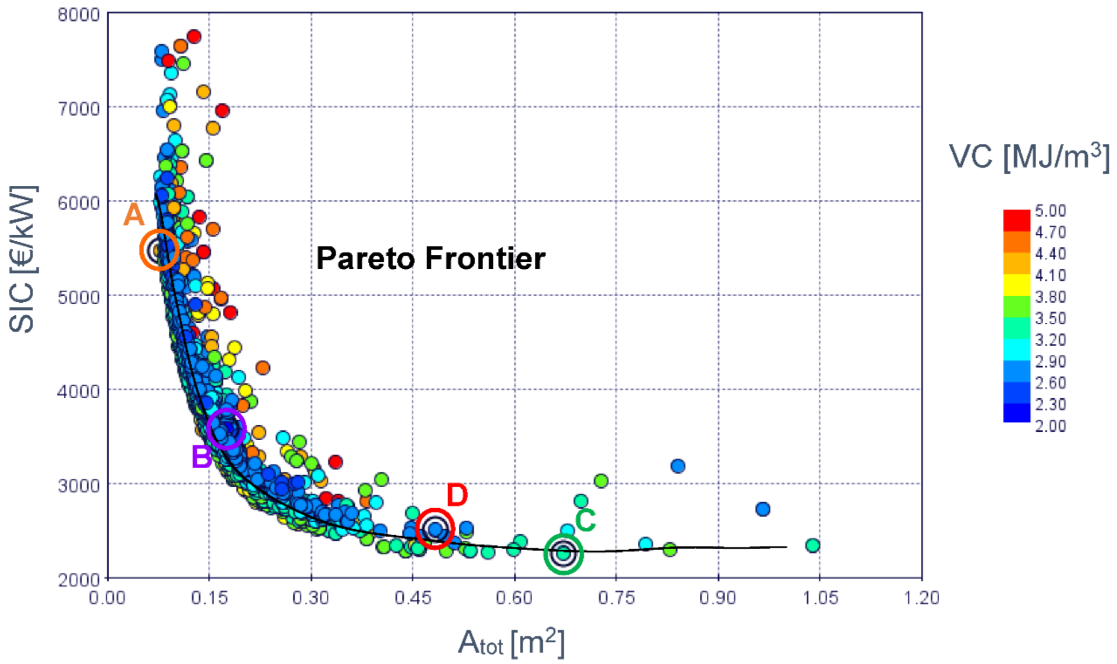

Fig 8. Optimization of Atot vs SIC

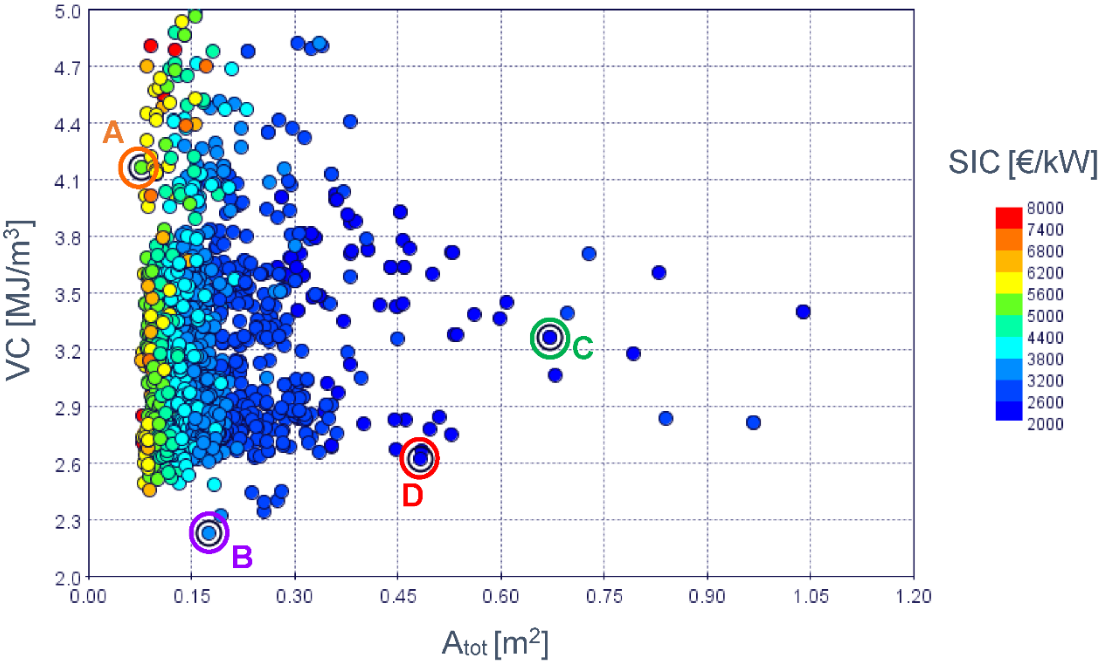

Fig 9. Optimization of Atot vs VC

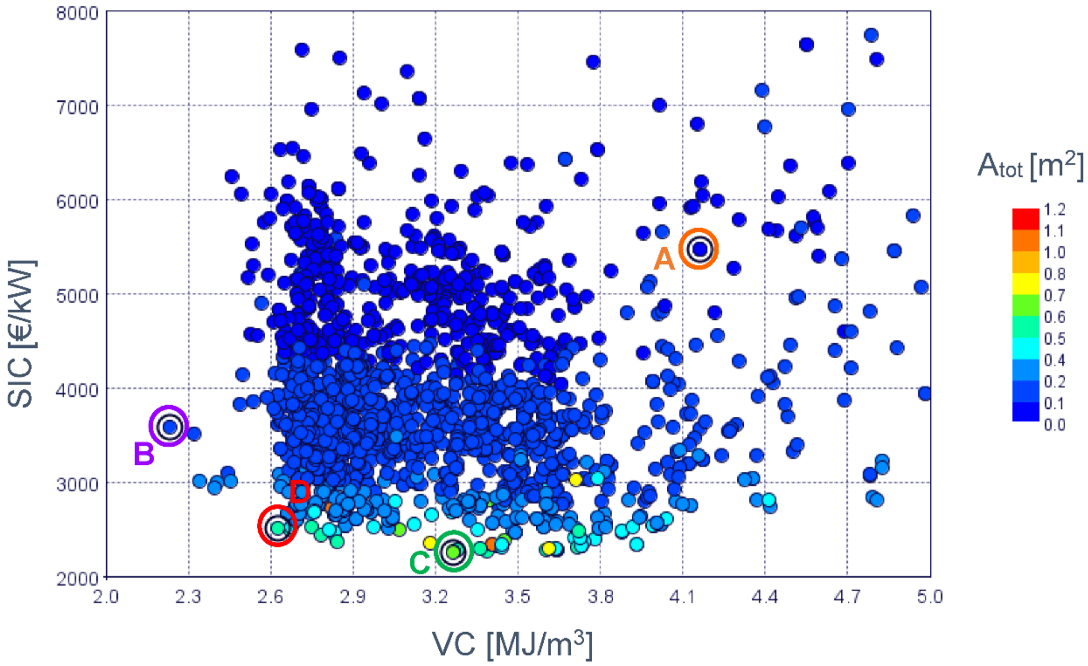

Fig 10. Optimization of VC vs SIC

Additionally, two parametric studies are present in order to compute the profitability of the project by means of the NPV and the PB. In order to compute the cash flows during the project, an estimation regarding fuel price and the number of hours should be made. As these factors present high level of uncertainty a parametric study is presented to take into account the variability of these parameters.

The cost of fuel has been initially estimated to 1€/l. However, due to ongoing fuel price changes, this parameter fluctuates over time. Fig 11 shows the evolution of PB and NPV with fuel price. PB indicates the period of years before the ORC system can produce a net profit [31]. NPV is a long-term financial tool which helps an individual or firm decide whether to make an investment. The pressure and superheating temperature are fixed to optimum ones obtained from the previous analysis.

Rising fuel prices from 0.6 to 2.4 €/l involve a reduction in the PB parameter from 8 to 2 years and an increase of NPV from -300€ to 11000€.

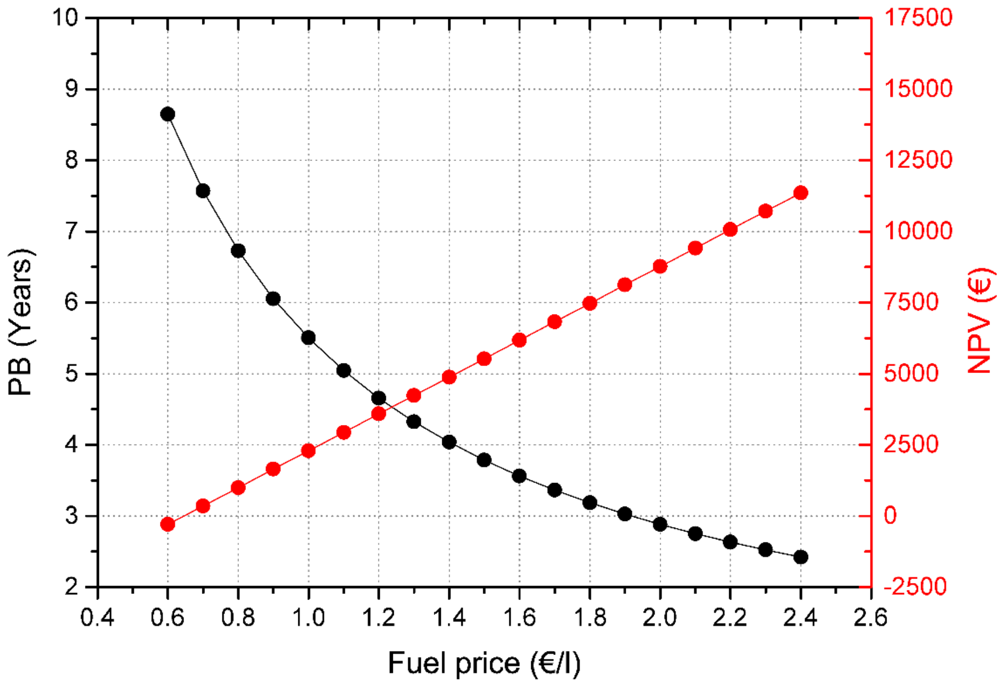

Fig 11. Evolution of Payback and NPV vs Fuel Price

The number of hours of an ORC operating in a year is estimated to 1100 h, which is approximately 3 hour per day. However, due to differences between countries, cities and vehicle users regarding the average time spent on a vehicle, a parametric study is presented in Fig 12.

Rising the number of hours per day from 0.5 h (182.5h per year) to 7.5 h (2737.5h per year) involves a reduction in the PB parameter from 18 to 2 years and an increase of NPV from -2500€ to 12500€. Therefore, both the fuel price and the number of hours running the ORC are critical parameters to consider in the payback estimation. This results in savings have a reasonable payback period [32] and lower risks comparing to other technologies [33].

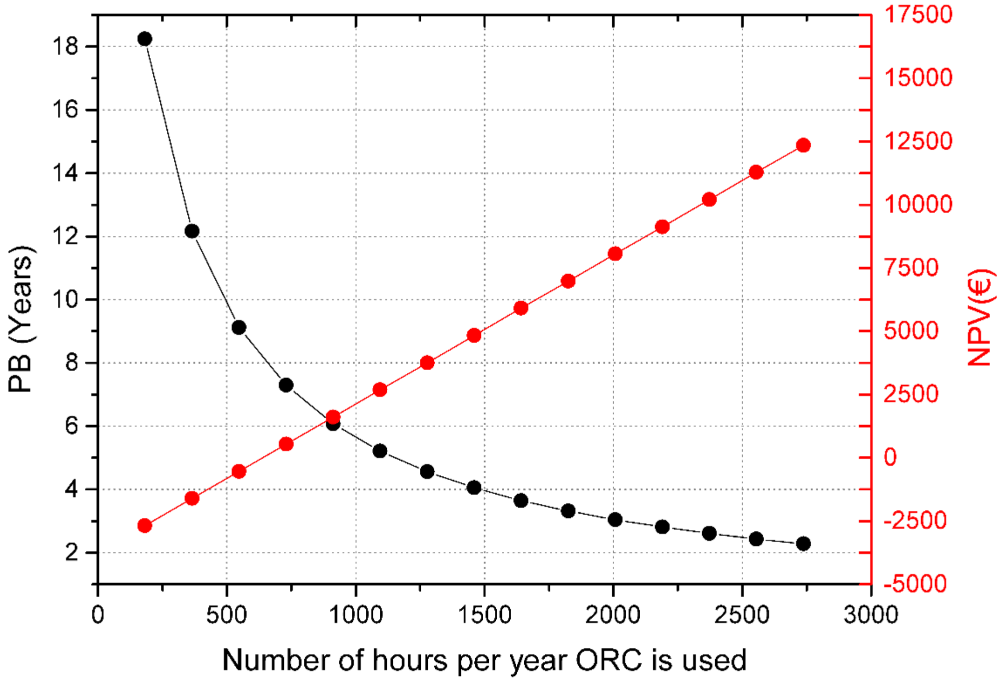

Fig 12. Evolution of Payback and NPV vs the number of hours the ORC is used

6. Conclusions

This paper presents a mathematical model of a bottoming ORC coupled to a 2l turbocharged gasoline engine to optimize the cycle from three different perspectives. Thermo-economic and sizing criteria are taken into account in this analysis.

The following results have been obtained:

1. SIC parameter increases up to a maximum value for the level of pressure in which the expander isentropic efficiency is maximum and for higher level of superheating temperature. The maximum value of the expander isentropic efficiency is fixed by the built-in volumetric expansion ratio. Considering the studied cycle, net power has a peak in the level of pressure between 28-30 bar and a degree of superheating temperature of 60ºC. Minimum value of SIC is approximately 2030 €/kW.
2. VC and A_{tot} are optimized at lower levels of superheating temperature and pressures between 28-32 bar. Higher levels of pressure and temperature of the working fluid reduce the pinch point in the evaporator, increasing the heat exchange area in the boiler. Regarding the expander, as the superheating temperature increases, the Volume Coefficient increases too. This parameter depends on the volumetric flow rate and the isentropic specific enthalpy drop through the expander. Higher superheating values imply higher levels of isentropic enthalpy drop and proportionally higher volume outlet flow rates across the expander.
3. A methodology to optimize ORC coupled to WHR systems in vehicle applications is presented using a multi-objective optimization algorithm

with thermo-economic and sizing criteria. These results show that the optimal solution depend on the importance of each objective to the final solution. Considering SIC as the main objective, greater heat exchangers area will be required. Considering sizing of the heat exchangers as the main objective, higher SIC will be obtained. Considering sizing of the expander (VC) as the main objective, higher SIC and heat exchanger areas will be obtained. Therefore, the Technique for Order Preference by Similarity to an Ideal Solution (TOPSIS) was implemented in order to take into account the preferences of the Decision Maker and select a single-solution from the Pareto frontier. Considering the weight factors as 0.5 for SIC, 0.3 for A_{tot} and 0.2 for VC and the boundaries of this particular application (an ORC coupled to a turbocharged engine in the 30 kW engine operating point), the result is optimized with values of 0.48 m^2 (A_{tot}), 2515 €/kW (SIC) and 2.62 MJ/m^3 (VC).

4. Two parametric studies are present in order to compute the profitability of the project by means of the NPV and the PB. In order to compute the cash flows during the project, an estimation regarding fuel price and the number of hours is presented. As these factors present high level of uncertainty a parametric study is presented to take into account the variability of these parameters. Rising fuel prices from 0.6 to 2.4 €/l involve a reduction in the PB parameter from 8 to 2 years and an increase of NPV from -300 € to 11000€. Rising the number of hours per day from 0.5 h (182.5h per year) to 7.5 h (2737.5h per year) involves a reduction in the PB parameter from 18 to 2 years and an increase of NPV from -2500€ to 12500€.

7. Acknowledgements

This work is part of a research project called “Evaluation of bottoming cycles in IC engines to recover waste heat energies” funded by a National Project of the Spanish Government with reference TRA2013-46408-R. Authors want to acknowledge the “Apoyo para la investigación y Desarrollo (PAID)” grant for doctoral studies (FPI S2 2015 1067). Authors acknowledge to ModeFRONTIER (ESTECO) because its support.

REFERENCES

[1] L. Arnaud, G. Ludovic, D. Mouad, Z. Hamid, and L. Vincent, “Comparison and Impact of Waste Heat Recovery Technologies on Passenger Car Fuel Consumption in a Normalized Driving Cycle,” *Energies*, vol. 7, no. 8, pp. 5273–5290, 2014.

[2] F. Payri, J. Luján, C. Guardiola, and B. Pla, “A Challenging Future for the IC Engine: New Technologies and the Control Role,” *Oil Gas Sci. Technol. – Rev. d’IFP Energies Nouv.*, vol. 70, pp. 15–30, 2014.

[3] H. Teng, G. Regner, and C. Cowland, “Waste Heat Recovery of Heavy-Duty Diesel Engines by Organic Rankine Cycle Part I: Hybrid Energy System of Diesel and Rankine Engines,” *SAE Int.*, vol. 1, no. 724, pp. 1–13, Apr. 2007.

[4] S. N. Hossain and S. Bari, “Waste heat recovery from the exhaust of a diesel generator using Rankine Cycle,” *Energy Convers. Manag.*, vol. 75, pp. 141–151, 2013.

[5] M. H. Yang and R. H. Yeh, “Thermodynamic and economic performances optimization of an organic Rankine cycle system utilizing exhaust gas of a large marine diesel engine,” *Appl. Energy*, vol. 149, pp. 1–12, 2015.

[6] C. Yue, F. You, and Y. Huang, “Thermal and economic analysis of an energy system of an ORC coupled with vehicle air conditioning,” *Int. J. Refrig.*, 2016.

[7] S. Quoilin, S. Declaye, B. F. Tchanche, and V. Lemort, “Thermo-economic optimization of waste heat recovery Organic Rankine Cycles,” *Appl. Therm. Eng.*, vol. 31, no. 14–15, pp. 2885–2893, 2011.

[8] J. Song and C. wei Gu, “Parametric analysis of a dual-loop organic Rankine cycle (ORC) system with wet steam expansion for engine waste heat recovery,” *Energy Convers. Manag.*, vol. 156, pp. 280–289, 2015.

[9] Z. Fergani, D. Touil, and T. Morosuk, “Multi-criteria exergy based optimization of an Organic Rankine Cycle for waste heat recovery in the

cement industry," *Energy Convers. Manag.*, vol. 112, pp. 81–90, 2016.

[10] G. Yu, G. Shu, H. Tian, H. Wei, and X. Liang, "Multi-approach evaluations of a cascade-Organic Rankine Cycle (C-ORC) system driven by diesel engine waste heat: Part B-techno-economic evaluations," *Energy Convers. Manag.*, vol. 108, pp. 579–595, 2015.

[11] L. Xiao, S. Y. Wu, T. T. Yi, C. Liu, and Y. R. Li, "Multi-objective optimization of evaporation and condensation temperatures for subcritical organic Rankine cycle," *Energy*, vol. 83, pp. 723–733, 2015.

[12] J. Wang, Z. Yan, M. Wang, S. Ma, and Y. Dai, "Thermodynamic analysis and optimization of an (organic Rankine cycle) ORC using low grade heat source," *Energy*, vol. 49, no. 1, pp. 356–365, 2013.

[13] V. L. Le, A. Kheiri, M. Feidt, and S. Pelloux-Prayer, "Thermodynamic and economic optimizations of a waste heat to power plant driven by a subcritical ORC (Organic Rankine Cycle) using pure or zeotropic working fluid," *Energy*, vol. 78, pp. 622–638, 2014.

[14] F. Yang, H. Zhang, C. Bei, S. Song, and E. Wang, "Parametric optimization and performance analysis of ORC (organic Rankine cycle) for diesel engine waste heat recovery with a fin-and-tube evaporator," *Energy*, vol. 91, pp. 128–141, 2015.

[15] J. Galindo, S. Ruiz, V. Dolz, L. Royo-Pascual, R. Haller, B. Nicolas, and Y. Glavatskaya, "Experimental and thermodynamic analysis of a bottoming Organic Rankine Cycle (ORC) of gasoline engine using swash-plate expander," *Energy Convers. Manag.*, vol. 103, pp. 519–532, Oct. 2015.

[16] J. Galindo, V. Dolz, L. Royo-Pascual, R. Haller, and J. Melis, "Modeling and Experimental Validation of a Volumetric Expander Suitable for Waste Heat Recovery from an Automotive Internal Combustion Engine Using an Organic Rankine," *Energies*, vol. 9, no. 279, pp. 1–18, 2016.

[17] B. Thonon, R. Vidil, and C. Marvillet, "Recent Research and Developments in Plate Heat Exchangers," *J. Enhanc. Heat Transf.*, vol. 2, no. 1–2, pp. 149–155, 1995.

[18] J. C. Chen, "Correlation for boiling heat transfer to saturated fluids in convective flow," *Ind. Eng. Chem. Process Des. Dev.*, vol. 5, no. 3, pp. 322–329, 1966.

[19] R. C. Lockhart, R.W., Martinelli, "Proposed Correlation of Data for Isothermal Two-Phase Two-Component Flow in Pipes," *Chem. Eng. Prog.*, vol. 45, pp. 39–48, 1949.

[20] Y. Y. Hsieh and T. F. Lin, "Saturated flow boiling heat transfer and pressure drop of refrigerant R-410A in a vertical plate heat exchanger," *Int. J. Heat Mass Transf.*, vol. 45, no. 5, pp. 1033–1044, 2002.

[21] W. S. Kuo, Y. M. Lie, Y. Y. Hsieh, and T. F. Lin, "Condensation heat transfer and pressure drop of refrigerant R-410A flow in a vertical plate heat exchanger," *Int. J. Heat Mass Transf.*, vol. 48, no. 25–26, pp. 5205–5220, 2005.

[22] J. R. García-Cascales, F. Vera-García, J. M. Corberán-Salvador, and J.

González-Maciá, “Assessment of boiling and condensation heat transfer correlations in the modelling of plate heat exchangers,” *Int. J. Refrig.*, vol. 30, no. 6, pp. 1029–1041, 2007.

[23] D. Maraver, J. Royo, V. Lemort, and S. Quoilin, “Systematic optimization of subcritical and transcritical organic Rankine cycles (ORCs) constrained by technical parameters in multiple applications,” *Appl. Energy*, vol. 117, pp. 11–29, 2014.

[24] E. S. Richardson, “Thermodynamic performance of new thermofluidic feed pumps for Organic Rankine Cycle applications,” *Appl. Energy*, vol. 161, pp. 75–84, 2016.

[25] S. Lecompte, S. Lemmens, H. Huisseune, M. Van Den Broek, and M. De Paepe, “Multi-objective thermo-economic optimization strategy for ORCs applied to subcritical and transcritical cycles for waste heat recovery,” *Energies*, vol. 8, no. 4, pp. 2714–2741, 2015.

[26] F. Heberle and D. Brüggemann, “Thermo-economic analysis of zeotropic mixtures and pure working fluids in organic rankine cycles for waste heat recovery,” *3rd Int. Semin. ORC Power Syst.*, vol. 53, pp. 1689–1699, 2013.

[27] C. M. Fonseca and P. J. Fleming, “Genetic Algorithms for Multiobjective Optimization: Formulation, Discussion and Generalization,” *Icga*, vol. 93, no. July, pp. 416–423, 1993.

[28] Y.-R. Li, J.-N. Wang, and M.-T. Du, “Influence of coupled pinch point temperature difference and evaporation temperature on performance of organic Rankine cycle,” *Energy*, vol. 42, no. 1, pp. 503–509, Jun. 2012.

[29] J. C. Ferreira, C. M. Fonseca, and A. Gaspar-Cunha, “Methodology to select solutions from the pareto-optimal set: A comparative study,” *Proc. GECCO 2007 Genet. Evol. Comput. Conf.*, pp. 789–796, 2007.

[30] Z. Yue, “A method for group decision-making based on determining weights of decision makers using TOPSIS,” *Appl. Math. Model.*, vol. 35, no. 4, pp. 1926–1936, 2011.

[31] X.-Q. Wang, X.-P. Li, Y.-R. Li, and C.-M. Wu, “Payback period estimation and parameter optimization of subcritical organic Rankine cycle system for waste heat recovery,” *Energy*, vol. 88, pp. 734–745, Aug. 2015.

[32] U. S. D. of Energy, “Waste Heat Recovery: Technology Opportunities in the US Industry,” *Waste Heat Recovery: Technology Opportunities in the US Industry*, pp. 1–112, 2008.

[33] M. Bailey, “Comparative Evaluation of Three Alternative Power Cycles for Waste Heat Recovery from the Exhaust of Adiabatic Diesel Engines,” *DOE NASA, United Technol. Res. Cent.*, vol. 86953, 1985.